European Journal of Medical Genetics 62 (2019) 103526

Contents lists available at ScienceDirect

European Journal of Medical Genetics

journal homepage: www.elsevier.com/locate/ejmg

A novel RAD21 p.(Gln592del) variant expands the clinical description of Cornelia de Lange syndrome type 4 – Review of the literature

Sanna Gudmundsson[a,*], Göran Annerén[a], Íñigo Marcos-Alcalde[b,c], Maria Wilbe[a], Malin Melin[a], Paulino Gómez-Puertas[b], Marie-Louise Bondeson[a,*]

[a] Department of Immunology, Genetics and Pathology, Uppsala University, Science for Life Laboratory, 75108, Uppsala, Sweden
[b] Centro de Biología Molecular "Severo Ochoa" (CSIC-UAM), 28049, Madrid, Spain
[c] Faculty of Experimental Sciences, Francisco de Vitoria University, Pozuelo de Alarcón, 28223, Madrid, Spain

ARTICLE INFO

Keywords:
RAD21 cohesin complex component
Cornelia de Lange syndrome type 4
Cohesin protein
Cohesin complex
Cohesinopathy

ABSTRACT

Cornelia de Lange syndrome (CdLS) is a heterogeneous developmental disorder where 70% of clinically diagnosed patients harbor a variant in one of five CdLS associated cohesin proteins. Around 500 variants have been identified to cause CdLS, however only eight different alterations have been identified in the *RAD21* gene, encoding the RAD21 cohesin complex component protein that constitute the link between SMC1A and SMC3 within the cohesin ring. We report a 15-month-old boy presenting with developmental delay, distinct CdLS-like facial features, gastrointestinal reflux in early infancy, testis retention, prominent digit pads and diaphragmatic hernia. Exome sequencing revealed a novel *RAD21* variant, c.1774_1776del, p.(Gln592del), suggestive of CdLS type 4. Segregation analysis of the two healthy parents confirmed the variant as *de novo* and bioinformatic analysis predicted the variant as disease-causing. Assessment by *in silico* structural model predicted that the p.Gln592del variant results in a discontinued contact between RAD21-Lys591 and the SMC1A residues Glu1191 and Glu1192, causing changes in the RAD21-SMC1A interface. In conclusion, we report a patient that expands the clinical description of CdLS type 4 and presents with a novel RAD21 p.(Glu592del) variant that causes a disturbed RAD21-SMC1A interface according to *in silco* structural modeling.

1. Introduction

Cornelia de Lange syndrome (CdLS) is characterized by cognitive impairment, growth deficiency, skeletal malformations, distinct facial features such as long eyelashes and thick highly arched eyebrows, and other major system deficiencies like gastrointestinal reflux. The patient group is heterogeneous with great variety in clinical manifestations and severity, primarily depending on which of the five CdLS associated cohesin proteins that are affected and the type of variant. Around 60% of clinically diagnosed CdLS patients harbor a Nipped B-like (*NIPBL*) variant, which results in a severe CdLS phenotype. Approximately 5% are diagnosed with a Structural maintenance of chromosomes 1A (*SMC1A*) variant, 5% with a Histone deacetylase 8 (*HDAC8*) variant and less then 1% harbor a variant in Structural maintenance of chromosome 3 (*SMC3*) or RAD21 cohesin complex component (*RAD21*). The remaning 30% of CdLS patients are without a genetic diagnosis. The cohesin complex is involved in DNA repair, transcriptional control and chromosome segregation, where RAD21, SMC1A and SMC3 constitute the cohesin ring that is responsible for sister chromatid adhesion during cell division (Fig. 1A) (Nasmyth and Haering, 2009). CdLS is thought to arise due to dysregulated transcription rather than deficient chromosome segregation (Dorsett, 2007). In total, around 500 variants affecting the cohesin complex have been associated to CdLS. However, only eight different alterations in *RAD21* have been identified to give rise to CdLS, referred to as CdLS type 4 (MIM #614701) (Boyle et al., 2015).

RAD21 was first associated to CdLS type 4 in four unrelated CdLS patients (Deardorff et al., 2012). Two patients had *de novo* deletions spanning *RAD21* (P1 and P4 in Fig. 1D) and two patients had *de novo* *RAD21* missense variants (c.1127C > G, p.Pro376Arg and c.1753T > C, p.Cys585Arg). Two previously reported patients diagnosed with Langer-Giedion syndrome (MIM #150230) were also highlighted as their clinical features overlapped with CdLS type 4 and they had deletions spanning *RAD21* (McBrien et al., 2008; Wuyts et al., 2002). In 2014, Minor et al. reported two patients, one with a frameshift variant (c.592_593dupAG, p.(Ser198Argfs*6)) of *de novo* or paternal origin, and one patient with a maternally inherited deletion spanning exon 13. The mother displayed very mild CdLS features

* Corresponding authors. Biomedical Center, Uppsala University, Box 815, 75108, Uppsala, Sweden.
E-mail addresses: sanna.gudmundsson@igp.uu.se (S. Gudmundsson), marielouise.bondeson@igp.uu.se (M.-L. Bondeson).

https://doi.org/10.1016/j.ejmg.2018.08.007
Received 6 March 2018; Received in revised form 14 August 2018; Accepted 15 August 2018
Available online 17 August 2018
1769-7212/

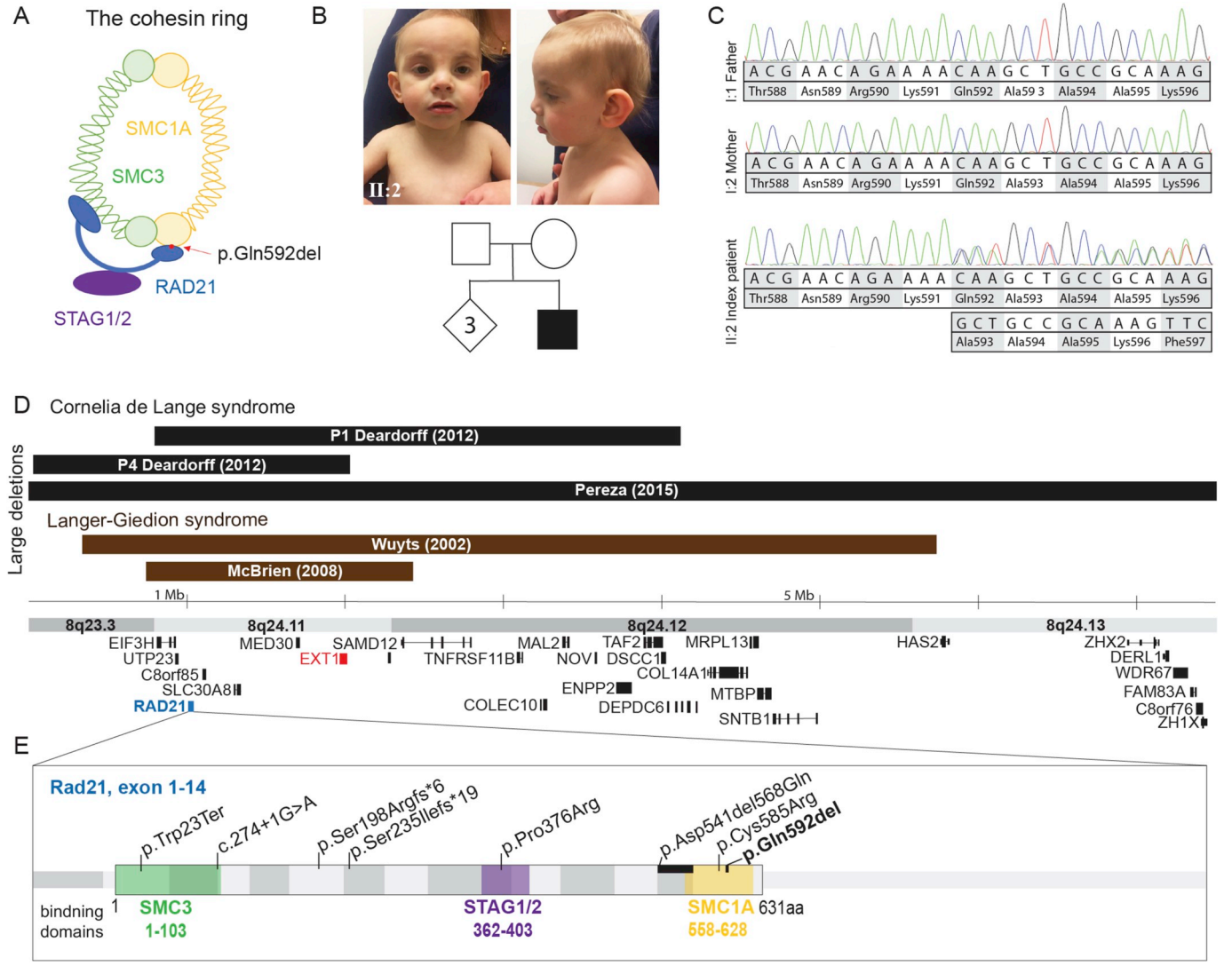

Fig. 1. Overview of patient features and RAD21 properties. (A) The RAD21 protein (blue) serves as a link between SMC3 protein (green) and SMC1A protein (yellow) that form the cohesin ring, responsible for adhesion of the sister chromatids during cell division, and involved in DNA repair and transcriptional control. The position of the p.Gln592del variant is indicated by a red arrow. (B) The index patient presented with Cornelia de Lange syndrome phenotype. Parents and the three older siblings were healthy. (C) A novel *de novo RAD21* c.1774_1776del, p.(592del) variant was confirmed in the index patient (II:2). (D) Three studies report deletions spanning *RAD21* in patients with Cornelia de Lange syndrome type 4 (black bars). Two patients with deletions spanning *RAD21* have been reported with Langer-Giedion syndrome (brown bars). (E) RAD21 is a 631 amino acid long protein with three binding domains: SMC3 (green, p.1–103), STAG1/2 (purple, p.362–403) and SMC1A (yellow, p.558–628). Previously reported intragenic variants are marked as well as the novel p.(Gln592del) variant identified in the index patient (bold). (For interpretation of the references to color in this figure legend, the reader is referred to the Web version of this article.)

(Minor et al., 2014). Ansari et al. also reported a familial case where an unaffected father had passed on a splice donor variant (c.274 + 1G > A) to his affected daughter (Ansari et al., 2014). In 2017, Boyle et al. report a frameshift variant, c.704delG, p.(Ser235Ilefs*19), in four related females (Boyle et al., 2017) and Martínez et al. identified a *de novo* c.68G > A, p.(Trp23Ter) variant in a boy (Martinez et al., 2017) (Fig. 1E).

Herein, we expand the clinical description of CdLS type 4 by reporting the clinical features of a 15-month-old boy with a novel variant in *RAD21*. We also highlight the effect of the variant by *in silico* structural modeling.

2. Clinical report

The patient was the fourth child of healthy non-related parents. He was born by caesarean section with a normal birthweight (3460 g). He presented with left sided congenital diaphragmatic hernia causing protruding of small intestine, stomach, spleen and part of colon to the thorax cavity, which was surgically treated two days post-delivery. He had gastroesophageal reflux disease during infancy and retention of the left testicle, which was surgically treated at 14 months of age. At 15 months he had the following features: distinct facial morphology, microcephaly (−3 SD), growth delay (length −1.5 SD, weight −3.5 SD) and developmental delay (Fig. 1B; Table 1). He displayed prominent digit pads on all fingers and a single transvers palmar crease. No hearing impairment or malformations of distal limbs were noted and there were no epileptic seizures. The patient occasionally took a few steps and could speak three words.

3. Methods

3.1. Ethical consent

The study was performed according to the Declaration of Helsinki

Table 1
Clinical features reported in the index patient and/or > 2 previously described Cornelia de Lange type 4 patients with distinct variants in RAD21.

Clinical features	Index patient	Previously reported patients (tot 13)[†]
CdLS-like facial features		
Synophrys	–	9
Thick and highly arched eyebrow	+	11
Long and prominent eyelashes	+	6
Short nose and nares anteverted	+	9
Wide or depressed nasal bridge	–	6
Long philtrum	–	9
Upper and lower lip thin vermilion	–	8
Macrotia	+	6 (4)
Ptosis	+	3
High or submucous cleft palate	+	3
Low-set or/and posterior angulation increased ear	+	3
Micrognathia	+	2
Developmental delay or intellectual disability	+	12 (1)
Microcephaly	+	10
Gastroesophageal reflux disease	+	7
Short stature	+	3 (2)
Abnormality of the genital system	+	2
Bridged or single transverse palmar crease	+	3
Prominent digit pad	+	0
Diaphragmatic hernia	+	0
5th finger clinodactyly	–	8 (1)
Low birth weight/Decreased body weight	–	5
Dislocated elbow/Abnormal extension	–	5
Sparse scalp hair	–	3
Toe cutaneous syndactyly	–	3 (1)
Exostoses [‡]	–	3

[+] Observed in the index patient, II:2. [–] Not observed in the index patient. [†] Clinical features reported in > 2 patients with different variants: number of affected patients (patients reported with normal feature). [‡] Suggestively associated to *EXT1* deletions and not *RAD21* variants.

guidelines after approval by the local ethics committee, Uppsala (Dnr, 2012/321) and collection of informed consent.

3.2. Whole-exome sequencing and segregation analysis

Whole-exome sequencing (WES) and analysis protocols, developed by the Clinical genomics facility in Uppsala, were adapted as a clinical WES test at the Department of Clinical Genetics, Uppsala University Hospital, Sweden. Briefly, genomic DNA from the trio was extracted from peripheral blood using automated systems (EZ1 and QIAsymphony, QIAGEN) according to standard protocols. For library preparation with Clinical Research Exome and SureSelectQXT Target Enrichment System (Agilent Technologies, Santa Clara, CA, USA) 250 ng DNA was used. Sequencing was performed with 150 base pair long paired-end reads on a NextSeq500 sequencer (Illumina, San Diego, CA). Alignment of raw data to the human reference genome (GRCh37/hg19) was performed using BWA 0.7.10 and variant calling was performed with GATK haplotype caller (GATK framework 3.2.4, GenomeAnalysisTK 3.2.2) by using the Bcbio-Nextgen pipeline v 0.8.9 (https://github.com/chapmanb/bcbio-nextgen). Quality control parameters were calculated using FastQC 0.11.2, Picard HsMetrics 1.96 (http://broadinstitute.github.io/picard/) and GATK Depth of Coverage (GATK framework 3.2.4, GenomeAnalysisTK 3.2.2). For filtering of variants BenchLab NGS (Agilent Technologies, Inc.) was used, including population frequency, phenotype data from the Human Gene Mutation Database Professional and ClinVar database. The allelic variants identified were classified according to the American College of Medical Genetics and Genomics and the Association for Molecular Pathology (Richards et al., 2015). The candidate variant was confirmed by Sanger sequencing of the family trio according to standard protocols (available upon request).

3.3. Three-dimensional structure modeling

The template structure was a stabilized model of human RAD21-Cterminal domain linked to the head domains of human SMC1A/SMC3 heterodimer, which was based on the structure of the C-terminal domain of yeast Scc1 protein (RAD21 in human) bound to yeast Smc1 homodimer (Protein Data Bank ID: 1W1W) (Haering et al., 2004), as previously described by Marcos-Alcalde et al. (2017). Model coordinates were built using the SWISS-MODEL server (http://swissmodel.expasy.org) and their structural quality was within the range of those accepted for homology-based structure (Anolea/Gromos/QMEAN4) (Benkert et al., 2011). To optimize geometries, the model was energy minimized using the GROMOS 43B1 force field implemented in DeepView (http://spdbv.vital-it.ch/), using 500 steps of steepest descent minimization followed by 500 steps of conjugate-gradient minimization. Figures were generated using the Pymol Molecular Graphics System (Schrödinger, LLC). Multiple sequence alignment of proteins from the RAD21 family was generated using TCOFFEE (http://www.tcoffee.org/) (Notredame et al., 2000).

4. Results

4.1. Whole-exome sequencing revealed a novel RAD21 c. 1774_1776del, p.(Gln592del) variant

WES was performed on the family trio with 93% of the reads mapping to the reference genome, at an average read depth of 159× and > 10× for 97% of the exome in the index patient. Filtering of trio

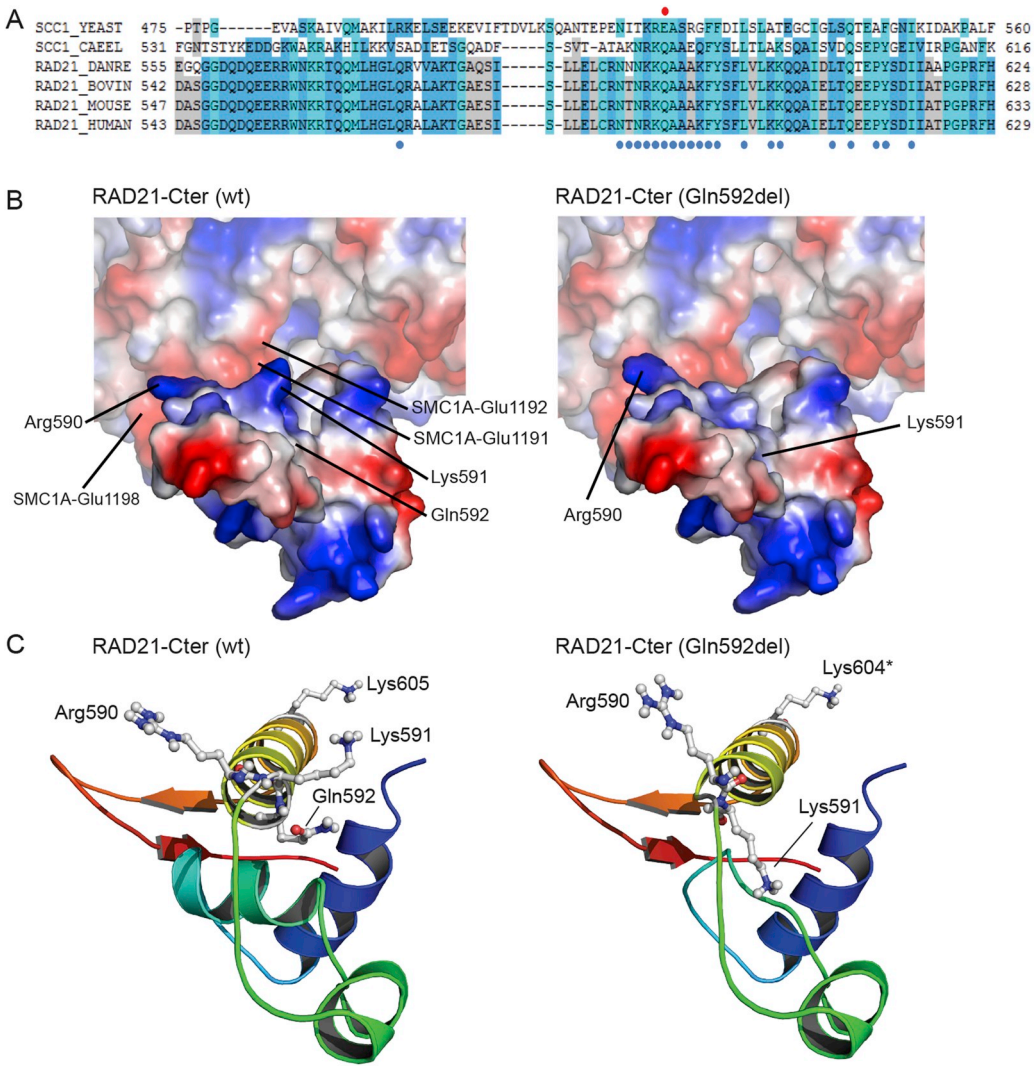

Fig. 2. *In silico* modeling of Gln592del mutant. (A) Multiple sequence alignment display conservation of the C-terminal domain of RAD21 (colored according to BLOSUM62 score). Dots indicate RAD21 residues connecting with SMC1A (blue) and the position of the deletion, p.Gln592 (red). (B) The surface of the structure model for wild-type RAD21-Cterminal domain (left) and for RAD21-Cterminal domain with p.Gln592del (right) is colored according to electrostatic characteristics (red: negative, blue: positive, white: neutral). Positively charged amino acid Arg590, interacting with SMC1A residue Glu1198, is affected by the p.Gln592 deletion. Lys591 has lost its connection to SMC1A residues Glu1191 and Glu1192. (C) Structure model for wild-type RAD21-Cterminal domain (left) and for RAD21-Ceterminal domain with p.Gln592del (right) with residues Arg590, Lys591, Gln592 and Lys605/Lys604* labeled. Lys591 residue have repositioned to the space previously occupied by the deleted Gln592 residue. (For interpretation of the references to color in this figure legend, the reader is referred to the Web version of this article.)

variants revealed heterozygosity for a novel *RAD21* variant, c.1774_1776del, p.(Gln592del), chr8:117859859_117859861delTTG (NM_006265) that was confirmed *de novo* in the index patient (Fig. 1C). The variant is not reported in the population of ExAC, GnomAD or SweGen databases (Ameur et al., 2017; Lek et al., 2016). ExAC database revealed that the level of observed missense variants in *RAD21* is lower than expected (ExAC: z = 2.76). Further, there is only one homozygous missense variant reported (p.Asp414Glu, rs75160167, n = 3), and no homozygous loss-of-function variants reported in the population databases (GnomAD, ExAC and SweGen). The patient phenotype and variant data has been submitted to ClinVar (https://www.ncbi.nlm.nih.gov/clinvar/), accession number SCV000747141.

4.2. *In silico modeling displayed changes in the p.Gln592del RAD21-SMC1A interface*

The p.Gln592del variant is located in the C-terminal of the last exon (14/14) within the SMC1A binding domain of RAD21 (p.558–628; Fig. 1E). The three-nucleotide position of the variant is conserved (PhyloP score 4.2; Fig. 2A) and the deletion is predicted to be deleterious (PROVEAN: −11.124) and disease causing (MutationTaster). Amino acids Arg590, Lys591 and Gln592 are located in a positively charged environment in close contact to the negatively charged residues Glu1198, Glu1191 and Glu1192 from the head domain of SMC1A (Fig. 2B, left). Deletion of Gln592 results in rearrangement of the surrounding residues. In particular, the structural model predicts a significant positional change of Lys591, now located in the space previously occupied by Gln592. As a result, the previous contact between Lys591 and the SMC1A residues Glu1191 and Glu1192 is discontinued, causing significant changes in the RAD21-SMC1A interface (Fig. 2B, right).

Residues Arg590, Lys591 and Gln592 are located in the same alpha helix as Lys605 (Fig. 2C, left). Lys605 is a key residue for the ATPase activity of the active site 1 of the cohesin ring, as it stabilizes the position of the SMC1A residues Asn34 and Gly35 in contact to ATP and the catalytic water molecule (Marcos-Alcalde et al., 2017). The change in the contact area between positive and negative patches on the interaction surface of RAD21 and SMC1A is expected to generate a local disorganization of the interface, thus affecting p.Lys605 and subsequently the ATPase-dependent functionality of the cohesin head (Fig. 2C, right).

5. Discussion

We report clinical and genetic findings of a boy with CdLS type 4, a syndrome of which clinical features of only 13 patients have been described in the literature before (Table 1). The index patient presented with clinical characteristics previously associated to CdLS type 4 as well as diaphragmatic hernia, which has been reported in about 1% of CdLS patients (Cunniff et al., 1993; Fryns, 1987; Jelsema et al., 1993; Marino et al., 2002; Pankau and Janig, 1993) but not in CdLS type 4 patients. The index patient also presented with prominent digit pads that has not

been reported in CdLS patients before but has been reported in a patient with a deletion spanning *RAD21* (McBrien et al., 2008) that shared clinical features with CdLS type 4 but was diagnosed with Langer-Giedion syndrome (Deardorff et al., 2012). Of note, exostoses, reported in three CdLS type 4 patients with micro deletions spanning *EXT1* (Table 1; Fig. 1D) (Deardorff et al., 2012; Pereza et al., 2015), are most likely not associated to CdLS type 4 and *RAD21* variants but caused by *EXTI* deletions as described before (MIM #133700).

The index patient was diagnosed with a novel *de novo RAD21* c.1774_1776, p.(Gln592del) variant. The affected p.Gln592 residue is conserved and the deletion is predicted to be deleterious and disease-causing. Further, the p.Gln592del variant is not reported in publically available databases and missense variants in *RAD21* in the normal population are underrepresented, suggesting that variants in *RAD21* might be disease-causing. The lack of homozygous loss-of-function variants in the normal population suggests that complete loss of RAD21 might be lethal. Previously, eight unique heterozygous alterations of *RAD21* variants have been reported in patients affected with CdLS type 4: three missense variants (Deardorff et al., 2012; Martinez et al., 2017), two frameshift variants (Boyle et al., 2017; Minor et al., 2014), one in-frame deletion including exon 13 of *RAD21,* one splice donor variant (Ansari et al., 2014) and deletions spanning whole *RAD21* (Deardorff et al., 2012; Pereza et al., 2015). Deardorff et al. has also highlighted two previously published patients, with deletions spanning *RAD21*, diagnosed with Langer-Giedion syndrome but with clinical symptoms overlapping CdLS type 4 (McBrien et al., 2008; Wuyts et al., 2002).

The RAD21 protein is a key unit of the cohesin complex, which is involved in chromosome segregation, DNA repair and transcriptional regulation (Dorsett, 2007; Nasmyth and Haering, 2009). Deletion of *RAD21* has been shown to result in haploinsufficiency (reduced *RAD21* RNA and RAD21 protein levels) but a disease-causing p.Pro376Arg variant did not affect the expression levels notably (Deardorff et al., 2012). Hence, different *RAD21* disease-causing variants suggestively act through different pathogenic mechanisms. It is clear that *RAD21* is sensitive to alterations and that variants can cause CdLS type 4, but there are also reports of heterozygous *RAD21* missense variants associated with chronic intestinal pseudo-obstruction, p.Ala622Thr (Bonora et al., 2015), and autism spectrum disorder, p.(Phe114Leu) (Yuen et al., 2015). The one-amino-acid deletion reported in this study is located in the C-terminal of RAD21 at the site responsible for SMC1A-head coupling (Haering et al., 2004). *In silico* modeling of RAD21 p.592del, display a clear structural change in residue Lys591 and, to a lesser extent, Arg590, which is predicted to affect the interface to SMC1A-head (Glu1191 and Glu1192). The p.592del variant is also suggested to influence RAD21 p.Lys605/Lys604 that facilitate a crucial function in ATP induced hydrolysis that is responsible for the opening of the cohesin molecule (Marcos-Alcalde et al., 2017). Therefore, we suggest that the function of the cohesin ring, and specifically the binding to SMC1A is altered, causing the phenotype observed in the patient.

In summary, we present a novel *RAD21* c.1774_1776del, p.(592del) variant, giving rise to CdLS type 4 in a boy. Segregation analysis, bioinformatic analysis, population data and *in silico* structural modeling vindicate the pathogenicity of this novel variant. This report summarizes previously reported clinical manifestations of CdLS type 4 but also highlights new clinical symptoms, which will aid counseling of future families affected with CdLS type 4.

Conflicts of interest

The authors have no conflicts of interest to declare.

Acknowledgments

We would like to thank the family for participating in this study. The study was supported by grants from Uppsala University Hospital as well as grants from the Spanish Ministry of Economy, Industry and Competitiveness (contracts IPT2011-0964-900000 and SAF2011-13156-E to P.G-P). SG was supported by grants from the Sävstaholm foundation.

References

Ameur, A., Dahlberg, J., Olason, P., Vezzi, F., Karlsson, R., Martin, M., Viklund, J., Kahari, A.K., Lundin, P., Che, H., Thutkawkorapin, J., Eisfeldt, J., Lampa, S., Dahlberg, M., Hagberg, J., Jareborg, N., Liljedahl, U., Jonasson, I., Johansson, A., Feuk, L., Lundeberg, J., Syvanen, A.C., Lundin, S., Nilsson, D., Nystedt, B., Magnusson, P.K., Gyllensten, U., 2017 Nov. SweGen: a whole-genome data resource of genetic variability in a cross-section of the Swedish population FEL. Eur. J. Hum. Genet. 25 (11), 1253–1260.

Ansari, M., Poke, G., Ferry, Q., Williamson, K., Aldridge, R., Meynert, A.M., Bengani, H., Chan, C.Y., Kayserili, H., Avci, S., Hennekam, R.C., Lampe, A.K., Redeker, E., Homfray, T., Ross, A., Falkenberg Smeland, M., Mansour, S., Parker, M.J., Cook, J.A., Splitt, M., Fisher, R.B., Fryer, A., Magee, A.C., Wilkie, A., Barnicoat, A., Brady, A.F., Cooper, N.S., Mercer, C., Deshpande, C., Bennett, C.P., Pilz, D.T., Ruddy, D., Cilliers, D., Johnson, D.S., Josifova, D., Rosser, E., Thompson, E.M., Wakeling, E., Kinning, E., Stewart, F., Flinter, F., Girisha, K.M., Cox, H., Firth, H.V., Kingston, H., Wee, J.S., Hurst, J.A., Clayton-Smith, J., Tolmie, J., Vogt, J., Tatton-Brown, K., Chandler, K., Prescott, K., Wilson, L., Behnam, M., McEntagart, M., Davidson, R., Lynch, S.A., Sisodiya, S., Mehta, S.G., McKee, S.A., Mohammed, S., Holden, S., Park, S.M., Holder, S.E., Harrison, V., McConnell, V., Lam, W.K., Green, A.J., Donnai, D., Bitner-Glindzicz, M., Donnelly, D.E., Nellaker, C., Taylor, M.S., FitzPatrick, D.R., 2014. Genetic heterogeneity in Cornelia de Lange syndrome (CdLS) and CdLS-like phenotypes with observed and predicted levels of mosaicism. J. Med. Genet. 51 (10), 659–668.

Benkert, P., Biasini, M., Schwede, T., 2011. Toward the estimation of the absolute quality of individual protein structure models. Bioinformatics 27 (3), 343–350.

Bonora, E., Bianco, F., Cordeddu, L., Bamshad, M., Francescatto, L., Dowless, D., Stanghellini, V., Cogliandro, R.F., Lindberg, G., Mungan, Z., Cefle, K., Ozcelik, T., Palanduz, S., Ozturk, S., Gedikbasi, A., Gori, A., Pippucci, T., Graziano, C., Volta, U., Caio, G., Barbara, G., D'Amato, M., Seri, M., Katsanis, N., Romeo, G., De Giorgio, R., 2015. Mutations in RAD21 disrupt regulation of APOB in patients with chronic intestinal pseudo-obstruction. Gastroenterology 148 (4) 771-782 e711.

Boyle, M.I., Jespersgaard, C., Brondum-Nielsen, K., Bisgaard, A.M., Tumer, Z., 2015. Cornelia de Lange syndrome. Clin. Genet. 88 (1), 1–12.

Boyle, M.I., Jespersgaard, C., Nazaryan, L., Bisgaard, A.M., Tumer, Z., 2017. A novel RAD21 variant associated with intrafamilial phenotypic variation in Cornelia de Lange syndrome - review of the literature. Clin. Genet. 91 (4), 647–649.

Cunniff, C., Curry, C.J., Carey, J.C., Graham Jr., J.M., Williams, C.A., Stengel-Rutkowski, S., Luttgen, S., Meinecke, P., 1993. Congenital diaphragmatic hernia in the Brachmann-de Lange syndrome. Am. J. Med. Genet. 47 (7), 1018–1021.

Deardorff, M.A., Wilde, J.J., Albrecht, M., Dickinson, E., Tennstedt, S., Braunholz, D., Monnich, M., Yan, Y., Xu, W., Gil-Rodriguez, M.C., Clark, D., Hakonarson, H., Halbach, S., Michelis, L.D., Rampuria, A., Rossier, E., Spranger, S., Van Maldergem, L., Lynch, S.A., Gillessen-Kaesbach, G., Ludecke, H.J., Ramsay, R.G., McKay, M.J., Krantz, I.D., Xu, H., Horsfield, J.A., Kaiser, F.J., 2012. RAD21 mutations cause a human cohesinopathy. Am. J. Hum. Genet. 90 (6), 1014–1027.

Dorsett, D., 2007. Roles of the sister chromatid cohesion apparatus in gene expression, development, and human syndromes. Chromosoma 116 (1), 1–13.

Fryns, J.P., 1987. [Posterolateral diaphragmatic hernia and Brachmann-de-Lange syndrome]. Arch. Fr. Pediatr. 44 (6), 474.

Haering, C.H., Schoffnegger, D., Nishino, T., Helmhart, W., Nasmyth, K., Lowe, J., 2004. Structure and stability of cohesin's Smc1-kleisin interaction. Mol. Cell 15 (6), 951–964.

Jelsema, R.D., Isada, N.B., Kazzi, N.J., Sargent, K., Harrison, M.R., Johnson, M.P., Evans, M.I., 1993. Prenatal diagnosis of congenital diaphragmatic hernia not amenable to prenatal or neonatal repair: Brachmann-de Lange syndrome. Am. J. Med. Genet. 47 (7), 1022–1023.

Lek, M., Karczewski, K.J., Minikel, E.V., Samocha, K.E., Banks, E., Fennell, T., O'Donnell-Luria, A.H., Ware, J.S., Hill, A.J., Cummings, B.B., Tukiainen, T., Birnbaum, D.P., Kosmicki, J.A., Duncan, L.E., Estrada, K., Zhao, F., Zou, J., Pierce-Hoffman, E., Berghout, J., Cooper, D.N., Deflaux, N., DePristo, M., Do, R., Flannick, J., Fromer, M., Gauthier, L., Goldstein, J., Gupta, N., Howrigan, D., Kiezun, A., Kurki, M.I., Moonshine, A.L., Natarajan, P., Orozco, L., Peloso, G.M., Poplin, R., Rivas, M.A., Ruano-Rubio, V., Rose, S.A., Ruderfer, D.M., Shakir, K., Stenson, P.D., Stevens, C., Thomas, B.P., Tiao, G., Tusie-Luna, M.T., Weisburd, B., Won, H.H., Yu, D., Altshuler, D.M., Ardissino, D., Boehnke, M., Danesh, J., Donnelly, S., Elosua, R., Florez, J.C., Gabriel, S.B., Getz, G., Glatt, S.J., Hultman, C.M., Kathiresan, S., Laakso, M., McCarroll, S., McCarthy, M.I., McGovern, D., McPherson, R., Neale, B.M., Palotie, A., Purcell, S.M., Saleheen, D., Scharf, J.M., Sklar, P., Sullivan, P.F., Tuomilehto, J., Tsuang, M.T., Watkins, H.C., Wilson, J.G., Daly, M.J., MacArthur, D.G., Exome Aggregation, C., 2016. Analysis of protein-coding genetic variation in 60,706 humans. Nature 536 (7616), 285–291.

Marcos-Alcalde, I., Mendieta-Moreno, J.I., Puisac, B., Gil-Rodriguez, M.C., Hernandez-Marcos, M., Soler-Polo, D., Ramos, F.J., Ortega, J., Pie, J., Mendieta, J., Gomez-Puertas, P., 2017. Two-step ATP-driven opening of cohesin head. Sci. Rep. 7 (1), 3266.

Marino, T., Wheeler, P.G., Simpson, L.L., Craigo, S.D., Bianchi, D.W., 2002. Fetal diaphragmatic hernia and upper limb anomalies suggest Brachmann-de Lange syndrome. Prenat. Diagn. 22 (2), 144–147.

Martinez, F., Caro-Llopis, A., Rosello, M., Oltra, S., Mayo, S., Monfort, S., Orellana, C., 2017. High diagnostic yield of syndromic intellectual disability by targeted next-generation sequencing. J. Med. Genet. 54 (2), 87–92.
McBrien, J., Crolla, J.A., Huang, S., Kelleher, J., Gleeson, J., Lynch, S.A., 2008. Further case of microdeletion of 8q24 with phenotype overlapping Langer-Giedion without TRPS1 deletion. Am. J. Med. Genet. 146A (12), 1587–1592.
Minor, A., Shinawi, M., Hogue, J.S., Vineyard, M., Hamlin, D.R., Tan, C., Donato, K., Wysinger, L., Botes, S., Das, S., Del Gaudio, D., 2014. Two novel RAD21 mutations in patients with mild Cornelia de Lange syndrome-like presentation and report of the first familial case. Gene 537 (2), 279–284.
Nasmyth, K., Haering, C.H., 2009. Cohesin: its roles and mechanisms. Annu. Rev. Genet. 43, 525–558.
Notredame, C., Higgins, D.G., Heringa, J., 2000. T-Coffee: a novel method for fast and accurate multiple sequence alignment. J. Mol. Biol. 302 (1), 205–217.
Pankau, R., Janig, U., 1993. Diaphragmatic defect in Brachmann-de Lange syndrome: a further observation. Am. J. Med. Genet. 47 (7), 1024–1025.
Pereza, N., Severinski, S., Ostojic, S., Volk, M., Maver, A., Dekanic, K.B., Kapovic, M., Peterlin, B., 2015. Cornelia de Lange syndrome caused by heterozygous deletions of chromosome 8q24: comments on the article by Pereza et al. [2012]. Am. J. Med. Genet. 167 (6), 1426–1427.
Richards, S., Aziz, N., Bale, S., Bick, D., Das, S., Gastier-Foster, J., Grody, W.W., Hegde, M., Lyon, E., Spector, E., Voelkerding, K., Rehm, H.L., Committee, A.L.Q.A., 2015. Standards and guidelines for the interpretation of sequence variants: a joint consensus recommendation of the American College of medical genetics and genomics and the association for molecular Pathology. Genet. Med. 17 (5), 405–424.
Wuyts, W., Roland, D., Ludecke, H.J., Wauters, J., Foulon, M., Van Hul, W., Van Maldergem, L., 2002. Multiple exostoses, mental retardation, hypertrichosis, and brain abnormalities in a boy with a de novo 8q24 submicroscopic interstitial deletion. Am. J. Med. Genet. 113 (4), 326–332.
Yuen, R.K., Thiruvahindrapuram, B., Merico, D., Walker, S., Tammimies, K., Hoang, N., Chrysler, C., Nalpathamkalam, T., Pellecchia, G., Liu, Y., Gazzellone, M.J., D'Abate, L., Deneault, E., Howe, J.L., Liu, R.S., Thompson, A., Zarrei, M., Uddin, M., Marshall, C.R., Ring, R.H., Zwaigenbaum, L., Ray, P.N., Weksberg, R., Carter, M.T., Fernandez, B.A., Roberts, W., Szatmari, P., Scherer, S.W., 2015. Whole-genome sequencing of quartet families with autism spectrum disorder. Nat. Med. 21 (2), 185–191.